

$O(\alpha^2 G_F m_t^2)$ Contributions to $H \rightarrow \gamma\gamma$

Yi Liao^a and Xiaoyuan Li^b

^a Department of Modern Applied Physics, Tsinghua University, Beijing 100084, P.R.China

^b Institute of Theoretical Physics, Chinese Academy of Sciences,

P.O.Box 2735, Beijing 100080, P.R.China

Abstract

The rare decay $H \rightarrow \gamma\gamma$ is a promising detection channel for an intermediate mass Higgs boson. We compute its two-loop $O(\alpha^2 G_F m_t^2)$ correction in the standard model and find that the relative correction to the decay rate runs between 0.7% and 0.5% for $M_H = 80 - 150$ GeV. The analogous correction to the amplitude for $gg \rightarrow H$ is recovered as a special case. The generalization of our result to other models is also briefly indicated.

Keywords: Higgs boson, rare decay, radiative correction

submitted to *Phys. Lett. B*

The standard model (SM) of the electroweak interactions [1] has proved very successful in the description of electroweak phenomenology. Yet, there is one particle, the Higgs boson, predicted by the SM that has evaded detection up to now. The Higgs boson is an essential ingredient of the SM. It provides mass for the W , Z bosons and fermions through the Higgs mechanism. Its discovery will thus be crucial for confirmation of the Higgs sector in the SM.

The search for the Higgs boson is difficult however. Theoretically this is basically because the relevant parameters such as masses, couplings are essentially free in the SM. Although there are theoretical considerations that can more or less constrain them our knowledge about these parameters is mainly from the failure search of experiments. For example, experiments at LEP I and SLC have ruled out the Higgs mass range $M_H \leq 63.5$ GeV at the 95% confidence level. It is expected that LEP II will extend the range up to 80 GeV. Beyond this we have to appeal to the next generation of hadron colliders. The production mechanisms for the Higgs boson at hadron colliders have been extensively studied in the literature [2]. Generally the gluon fusion mechanism [3] dominates for a Higgs mass up to 700 GeV. Above this range the dominant mechanism is through W , Z scattering subprocesses. The detection mechanisms for Higgs boson in the range $M_H \sim 140 - 800$ GeV have also been widely studied (see, for example, Refs.[2][4][5]). Less extensively studied is the so-called intermediate mass Higgs boson in the region $M_H \sim 80 - 140$ GeV [6]. It is difficult to detect a Higgs boson in this region because the dominant decay mode $H \rightarrow b\bar{b}$ is badly buried in the enormous QCD jet background[7] so that one has to use rare decays. A favorite decay mode is $H \rightarrow \gamma\gamma$, though an excellent energy resolution is still required to discriminate signals from the background produced from $q\bar{q}(gg) \rightarrow \gamma\gamma$ and fake γ 's from π^0 decays[4]. Since the signal of $H \rightarrow \gamma\gamma$ is so small and may be overwhelmed by the background it is important to predict its decay rate as precisely as possible.

At lowest order the amplitude for the decay $H \rightarrow \gamma\gamma$ receives contributions from charged fermion and W boson loops[8]. Among fermions in the SM, only the top quark is of practical importance in fermion loops[3]. The QCD correction to the top loop was considered in Ref. [9] and found to be well under control. The $O(\alpha^2 G_F m_t^2)$ correction from internal exchange of the Higgs boson in the top loop was computed in Ref. [10]. In this paper, we will complete this by including contributions from unphysical Goldstone bosons as well. The gluon fusion process $gg \rightarrow H$ is quite similar to the decay $H \rightarrow \gamma\gamma$. The QCD correction to the fusion was shown to be very large [11] and this would make the $O(G_F m_t^2)$ corrections relatively more important for $H \rightarrow \gamma\gamma$ than for $gg \rightarrow H$. The $O(\alpha_s^2 G_F m_t^2)$ correction to the fusion has been computed by the use of the low energy theorem for the trace of the energy-momentum tensor and found to be small[12]. Although the $O(\alpha_s^2 G_F m_t^2)$ correction for $gg \rightarrow H$ may be reproduced from that for $H \rightarrow \gamma\gamma$ by assigning equal charges to the top and bottom quarks, the latter cannot be obtained simply from the former as shown below.

The lowest order contribution to the amplitude for $H \rightarrow \gamma\gamma$ is

$$\begin{aligned} i\mathcal{A}_{t+w}^{1-\text{loop}} &= i\mathcal{O}[N_c Q_t^2 F_t + (Q_t - Q_b)^2 F_W], \\ \mathcal{O} &= \frac{\alpha}{2\pi v} \epsilon_\mu^*(1) \epsilon_\nu^*(2) (g^{\mu\nu} k_1 \cdot k_2 - k_2^\mu k_1^\nu), \end{aligned} \quad (1)$$

where $k_{1,2}$ and $\epsilon(1,2)$ are the momenta and polarization vectors of the two photons, $Q_{t,b}$ are the electric charges of the top and bottom quarks, N_c is the number of colors, and $v = 2^{-1/4} G_F^{-1/2} = 246$ GeV. F_t and F_W are functions of $\eta_t = 4m_t^2/M_H^2$ and $\eta_w = 4M_W^2/M_H^2$ respectively, given in Refs. [2][3][8]. To obtain the desired $O(\alpha^2 G_F m_t^2)$ correction, we work in the heavy top limit. This is a good approximation for an intermediate mass Higgs boson. In explicitly renormalizable R_ξ gauges, the leading term in this limit is provided by internal exchange of the Higgs and unphysical Goldstone bosons with minimal number of contact interactions amongst themselves. This is because the introduction of a contact scalar vertex will bring in a factor of $M_H^2 = 2k_1 \cdot k_2$ that cannot be cancelled by the possible logarithmic infrared behaviour of diagrams in the limit $m_t^2 \gg M_H^2$, and thus

will not contribute to the leading term. Furthermore, the non-leading terms are $\xi_{W,Z}$ -dependent, and this dependence is cancelled only when contributions from W , Z bosons are included. With these considerations, the relevant interaction Lagrangian is

$$\mathcal{L} = -\frac{m_t}{v}H\bar{t}t + i\frac{m_t}{v}\phi^0\bar{t}\gamma_5t + \sqrt{2}\frac{m_t}{v}(\phi^+\bar{t}_Rb_L + \phi^-\bar{b}_Lt_R) + eA_\mu(Q_t\bar{t}\gamma^\mu t + Q_b\bar{b}\gamma^\mu b) \quad (2) \\ + ie(Q_t - Q_b)A_\mu(\phi^-\partial^\mu\phi^+ - \phi^+\partial^\mu\phi^-) + e^2(Q_t - Q_b)^2A_\mu A^\mu\phi^+\phi^-,$$

where H , $\phi^{0,\pm}$ are the Higgs and unphysical Goldstone bosons respectively, and A_μ the photon field. We have ignored the small bottom mass and quark mixing.

The two-loop diagrams that may contain the desired correction are obtained by attaching in all possible ways the two photon lines onto the diagram shown in Fig. 1. They are shown in Fig. 2. These diagrams are classified into three groups. The first group corresponds to the insertion of the following one-loop elements in the one-loop top or bottom diagram for $H \rightarrow \gamma\gamma$: the top self-energy (denoted as W), the $Ht\bar{t}$ or $Hb\bar{b}$ vertex (V_1), and the $A_\mu t\bar{t}$ vertex (V_2 and V_3). The second group consists of the insertion of the one-loop $H\phi^+\phi^-$ vertex in the one-loop ϕ^\pm diagrams for $H \rightarrow \gamma\gamma$ (V_4). The third group is the remaining overlapping diagram (R). Note that diagrams $V_{3,4}$ and R are present only when the exchanged virtual scalars are the charged one, ϕ^\pm . It is these diagrams that will produce the difference between the $O(G_F m_t^2)$ corrections to $H \rightarrow \gamma\gamma$ and $gg \rightarrow H$.

The contributions from the H -, ϕ^0 - and ϕ^\pm -exchanged diagrams are respectively gauge invariant and can be calculated separately. In addition, parity is violated by the $\phi^\pm tb$ vertex so the ϕ^\pm -exchanged diagrams will generally induce a new parity-violating Lorentz structure, $O_{\mu\nu} = i\epsilon_{\mu\nu\rho\sigma}k_1^\rho k_2^\sigma$. Since the one-loop amplitude is symmetric and $O_{\mu\nu}$ antisymmetric with respect to μ and ν , the parity-violating term will not contribute to the total decay rate to the order considered here and may be safely ignored. In other words, there are no ambiguities associated with the γ_5 problem though we are computing two-loop diagrams.

Now we describe the renormalization procedures used to define the physical parameters and renormalization constants. We use the dimensional regularization to regulate ultravi-

olate divergences and work in the on-shell renormalization scheme. For our purpose, the mass of the unphysical Goldstone bosons can be set to zero from the very beginning, but with one caveat as explained below.

1. Mass and wavefunction renormalization of the top (W) – The counterterms for the top mass (δm_t) and wavefunction renormalization constant (δZ_t) are determined by requiring that m_t be the pole of the one-loop corrected propagator of the top and that the residue of the propagator at its pole be unity. Note that in the case of ϕ^\pm exchange there are wavefunction renormalization constants for the left- and right-handed parts respectively, $Z_t^L = 1 + \delta Z_t^L$, $Z_t^R = 1 + \delta Z_t^R$.

2. Renormalization of the $Ht\bar{t}$ and $Hb\bar{b}$ vertices (V_1) – In the SM, this is not independent but is related to the renormalization of the t , b self-energy. The Feynman rule for the counterterm of the $Ht\bar{t}$ vertex induced by H – or ϕ^0 –exchange is $-im_t/v(\delta m_t/m_t + \delta Z_t)$. For ϕ^\pm exchange there is no counterterm for the $Hb\bar{b}$ vertex in the limit of zero bottom mass, but there is a counterterm for the $Ht\bar{t}$ vertex, $-im_t/v(\delta m_t/m_t + 1/2(\delta Z_t^L + Z_t^R))$ though its bare one-loop diagram does not exist in this limit. Finally there is a global counterterm for the $Ht\bar{t}$ vertex, $(-im_t/v)(\delta v/v)$ where δv is the VEV counterterm of the Higgs field induced by the heavy top.

3. Renormalization of the $A_\mu t\bar{t}$ vertices ($V_{2,3}$) – The electric charge is defined as usual in the Thomson limit. We have checked that the $U(1)_{\text{e.m.}}$ Ward identity is satisfied especially in the case of ϕ^\pm –exchange where this is not self-evident.

4. Renormalization of the $H\phi^+\phi^-$ vertex (V_4) – The computation of diagrams V_4 requires special care. Let us first discuss the renormalization of the vertex. The counterterm for the vertex is $-i(M_H^2/v)(\delta Z_\lambda - \delta v/v)\mu^\epsilon$, where δZ_λ is the renormalization constant for the scalar self-coupling λ , $\delta Z_\lambda = \delta Z_H + (1/M_H^2)(\delta M_H^2 - \delta M_{\phi^\pm}^2) + 2\delta v/v$. The mass and wavefunction renormalization of the Higgs boson (δM_H^2 , δZ_H) is done as for the top so that there is no renormalization factor for the external Higgs boson. The counterterm

for the mass of ϕ^\pm ($\delta M_{\phi^\pm}^2$) is determined by the condition of tadpole cancellation at the one-loop level. The masslessness of $\phi^{0,\pm}$ is then automatically preserved by the Goldstone theorem at the same level. Since the counterterm for V_4 is to be inserted into a finite one-loop amplitude and only terms up to $O(m_t^2)$ are required, we obtain

$$-i\frac{M_H^2}{v}(\delta Z_\lambda - \delta v/v)\mu^\epsilon = i\mu^\epsilon 8N_c \frac{m_t^2}{v} \left(\frac{m_t}{4\pi v}\right)^2 [\Delta_\epsilon - \frac{7}{48} \frac{M_H^2}{m_t^2}], \quad \Delta_\epsilon = \Gamma(\epsilon) + \ln \frac{4\pi\mu^2}{m_t^2}, \quad (3)$$

where $\frac{\delta v}{v} = \frac{7}{6}N_c \left(\frac{m_t}{4\pi v}\right)^2$ has been inserted.

It is straightforward to calculate the contributions from H – or ϕ^0 -exchanged diagrams, i.e., diagrams W and $V_{1,2}$. The bare H-exchanged diagrams sum to a finite, gauge invariant form. In the heavy top limit, it is given by

$$i\mathcal{A}_{H(\text{bare})}^{2\text{-loop}} = i\mathcal{O}N_c \left(\frac{m_t}{4\pi v}\right)^2 [-6Q_t^2]. \quad (4)$$

The counterterm diagrams as a whole are also finite and gauge invariant,

$$i\mathcal{A}_{H(\text{c.t.})}^{2\text{-loop}} = \delta m_t^{(H)} \frac{\partial}{\partial m_t} i\mathcal{A}_t^{1\text{-loop}} = i\mathcal{O}N_c \left(\frac{m_t}{4\pi v}\right)^2 [4Q_t^2], \quad (5)$$

where $\delta m_t^{(H)}$ is the counterterm for the top mass induced by H-exchange, and $i\mathcal{A}_t^{1\text{-loop}}$ must be computed in n -dimensions, i.e.,

$$F_t = -\frac{4}{3}\Gamma(1+\epsilon)\mu^\epsilon \left(\frac{4\pi\mu^2}{m_t^2}\right)^\epsilon. \quad (6)$$

Note that the wavefunction renormalization constant for the top is cancelled. Similarly, we obtain,

$$\begin{aligned} i\mathcal{A}_{\phi^0(\text{bare})}^{2\text{-loop}} &= i\mathcal{O}N_c \left(\frac{m_t}{4\pi v}\right)^2 \left[\frac{14}{3}Q_t^2\right], \\ i\mathcal{A}_{\phi^0(\text{c.t.})}^{2\text{-loop}} &= \delta m_t^{(\phi^0)} \frac{\partial}{\partial m_t} i\mathcal{A}_t^{1\text{-loop}} = i\mathcal{O}N_c \left(\frac{m_t}{4\pi v}\right)^2 \left[-\frac{4}{3}Q_t^2\right]. \end{aligned} \quad (7)$$

It is much more difficult to calculate the contributions from ϕ^\pm -exchanged diagrams. Besides W , $V_{1,2,3}$ and R , they involve V_4 that are seemingly infrared divergent in the limit of massless ϕ^\pm . Although they are actually not infrared divergent, individual diagrams do contain terms that are non-analytic in $p^2 = 2k_1 \cdot k_2$ (Higgs boson momentum squared

), like $g_{\mu\nu} \ln^n \frac{p^2}{m_t^2}$ ($n = 1, 2$), $g_{\mu\nu} \frac{p^2}{m_t^2} \ln \frac{p^2}{m_t^2}$, $\frac{k_{2\mu}k_{1\nu}}{p^2}$, $\frac{k_{2\mu}k_{1\nu}}{p^2} \ln \frac{p^2}{m_t^2}$ and $k_{2\mu}k_{1\nu} \ln \frac{p^2}{m_t^2}$. It is a non-trivial check of our calculation that these terms are cancelled in the sum of two diagrams in V_4 so that they will not spoil our low energy expansion in the heavy top limit. The imaginary part is also cancelled in the sum. This is reminiscent of the observation that the one-loop ϕ^\pm -exchanged amplitude for $H \rightarrow \gamma\gamma$ does not contain an imaginary part in the limit of massless ϕ^\pm . The sum of all bare ϕ^\pm -exchanged diagrams and the counterterms for V_4 is

$$i\mathcal{A}_{\phi^\pm(\text{bare})}^{2\text{-loop}} = i\mathcal{O}N_c(\frac{m_t}{4\pi v})^2[(4Q_tQ_b - \frac{8}{3}Q_t^2) + 5(Q_t - Q_b)^2], \quad (8)$$

where the second term is contributed by diagrams V_4 and counterterms, and the first term is contributed by other bare diagrams. We note that diagrams V_4 actually contain an additional term proportional to $(Q_t - Q_b)^2 g_{\mu\nu}[-1 - 4\Delta_{2\epsilon} - \frac{2}{3}\frac{p^2}{m_t^2}]$, which is exactly cancelled by other diagrams. The remaining counterterms also sum to a gauge invariant form,

$$i\mathcal{A}_{\phi^\pm(\text{c.t.})}^{2\text{-loop}} = \delta m_t^{(\phi^\pm)} \frac{\partial}{\partial m_t} i\mathcal{A}_t^{1\text{-loop}} = i\mathcal{O}N_c(\frac{m_t}{4\pi v})^2[\frac{4}{3}Q_t^2]. \quad (9)$$

Notice that the wavefunction renormalization constants δZ_t^L and δZ_t^R are again cancelled in the sum. This is because the absence of a counterterm for the $Hb\bar{b}$ vertex is compensated for by the presence of a counterterm for the $Ht\bar{t}$ vertex. The same counterterm also makes the $\delta m_t^{(\phi^\pm)}$ part just as simple as in the case of H or ϕ^0 exchange.

Finally, there is a contribution from the counterterm $\delta v/v$ for the $Ht\bar{t}$ vertex,

$$i\mathcal{A}_{\delta v}^{2\text{-loop}} = \frac{\delta v}{v} i\mathcal{A}_t^{1\text{-loop}} = i\mathcal{O}N_c(\frac{m_t}{4\pi v})^2[-\frac{14}{9}N_cQ_t^2]. \quad (10)$$

Three different methods are employed to compute two loop diagrams. (1) After loop integration we expand Feynman parameter integrals in the heavy top limit to obtain the $g_{\mu\nu}$ and $k_{2\mu}k_{1\nu}$ terms. (2) We slightly modify the Hoogeveen's method on expansion in the large mass limit[13]. We directly expand top propagators to the desired order without

shifting γ matrices from denominators to numerators beforehand, and then use algebraic identities to further reduce their products. This simplifies algebra considerably. We use this to get the $k_{2\mu}k_{1\nu}$ terms. (3) After loop integration we use numerical analysis to approach the heavy top limit. Both $g_{\mu\nu}$ and $k_{2\mu}k_{1\nu}$ terms are computed. In the case of H-exchange all three methods lead to an identical result. For ϕ^0 -exchanged diagrams we use the first two methods and indeed obtain the same numbers. It is complicated to apply the method (2) to ϕ^\pm -exchanged diagrams due to the infrared behaviour associated with masslessness of the bottom and ϕ^\pm , so only the method (1) is used. But even so, we still have nontrivial checks as mentioned above: cancellation of non-analytic terms in diagrams V_4 , and cancellation of divergent, non-gauge-invariant terms proportional to $g_{\mu\nu}(Q_t - Q_b)^2$ between V_4 and other diagrams. To summarize, the complete $O(\alpha^2 G_F m_t^2)$ contribution to the decay amplitude is

$$i\mathcal{A}^{2\text{-loop}} = i\mathcal{O}N_c\left(\frac{m_t}{4\pi v}\right)^2[4Q_tQ_b + 5(Q_t - Q_b)^2 - \frac{14}{9}N_cQ_t^2]. \quad (11)$$

The amplitude for the fusion $gg \rightarrow H$ is recovered by setting $Q_t = Q_b$ and changing coupling factors appropriately,

$$\begin{aligned} & i\mathcal{A}(g_a g_b \rightarrow H) \\ &= \frac{i\alpha_s}{2\pi v}\epsilon_\mu(1)\epsilon_\nu(2)(g^{\mu\nu}k_1 \cdot k_2 - k_2^\mu k_1^\nu)\text{tr}\left(\frac{\lambda_a}{2}\frac{\lambda_b}{2}\right)\left(-\frac{4}{3}\right)\left[1 + \left(\frac{m_t}{4\pi v}\right)^2(-3 + \frac{7}{6}N_c)\right] \\ &= \frac{i\alpha_s}{2\pi v}\epsilon_\mu(1)\epsilon_\nu(2)(g^{\mu\nu}k_1 \cdot k_2 - k_2^\mu k_1^\nu)\text{tr}\left(\frac{\lambda_a}{2}\frac{\lambda_b}{2}\right)\left(-\frac{4}{3}\right)\left[1 + \frac{\sqrt{2}G_F m_t^2}{32\pi^2}\right], \end{aligned} \quad (12)$$

which coincides with the result of Ref. [12].¹

Including $O(\alpha^2 G_F m_t^2)$ and QCD corrections, the decay rate for $H \rightarrow \gamma\gamma$ is

$$\Gamma = \Gamma_{1\text{-loop}}\left[1 + \frac{\sqrt{2}G_F m_t^2}{8\pi^2}B + \frac{2\alpha_s}{\pi}C\right], \quad (13)$$

where $\Gamma_{1\text{-loop}}$ is the lowest one loop contribution, C was computed in Ref. [9] and

$$B = N_c[4Q_tQ_b + 5(Q_t - Q_b)^2 - \frac{14}{9}N_cQ_t^2]/[N_cQ_t^2F_t + (Q_t - Q_b)^2F_W]. \quad (14)$$

¹We thank A. Djouadi for pointing out an error in our comments on Ref. [12] in the original version of this paper.

For numerical analysis we use $m_t = 176$ GeV, then the $O(\alpha^2 G_F m_t^2)$ correction to the decay rate runs between 0.7% and 0.5% for $M_H = 80 - 150$ GeV, which is roughly one half of the corresponding QCD correction[9] if $\alpha_s \sim 0.1$ is used.

The results reported here may be employed to incorporate contributions from exchange of extra scalars in models with an extended Higgs sector. For example, in the two Higgs doublet model [14] the contributions from all of the four physical scalars may be incorporated by multiplying appropriate factors coming from vertices. But it is suspect that the heavy top limit remains to be a good approximation as these particles are generally much heavier than the top quark.

We thank K.-T. Chao and Y.-P. Kuang for discussions.

References

- [1] S. Glashow, Nucl. Phys. 20 (1961) 579; S. Weinberg, Phys. Rev. Lett. 19 (1967) 1264; A. Salam, *in* Elementary Particle Theory, ed. by N. Southholm (Almquist and Wiksell, Stockholm, 1968)
- [2] For reviews, see e.g., E. Eichten, I. Hinchliffe, K. Lane and C. Quigg, Rev. Modern Phys. 56 (1984) 579; J. F. Gunion, H. Haber, G. L. Kane and S. Dawson, The Higgs Hunter's Guide (Addison-Wesley, Reading, 1990)
- [3] H. Georgi, S. L. Glashow, M. E. Machacek and D. V. Nanopoulos, Phys. Rev. Lett. 40 (1978) 692
- [4] Z. Kunszt and W. J. Stirling, Phys. Lett. B242 (1990) 507; R. Kleiss, Z. Kunszt and W. J. Stirling, *ibid* B253 (1990)269
- [5] W. J. Marciano and F. E. Paige, Phys. Rev. Lett. 66 (1991) 2433
- [6] Z. Kunszt, Nucl. Phys. B247 (1984) 339; J. F. Gunion, G. L. Kane and J. Wudka, *ibid* B299 (1988) 231
- [7] H. Baer and J. F. Owens, Phys. Lett. B205 (1988) 231
- [8] J. Ellis, M. K. Gaillard and D. V. Nanopoulos, Nucl. Phys. B106 (1976) 292

- [9] H. Zheng and D. Wu, Phys. Rev. D42 (1990) 3760; A. Djouadi, M. Spira, J. J. van der Bij and P. M. Zervas, Phys. Lett. B257 (1991) 187; K. Melnikov and O. Yakovlev, *ibid* B312 (1993) 179; A. Djouadi, M. Spira and P. Zervas, Phys. Lett. B311 (1993) 255; S. Dawson and R. Kauffman, Phys. Rev. D47 (1993) 1264
- [10] Yi Liao, PhD Thesis, Jan. 1994, Institute of Theoretical Physics, Chinese Academy of Sciences, Beijing (unpublished)
- [11] A. Djouadi, M. Spira and P. M. Zervas, Phys. Lett. B264 (1991) 440; S. Dawson, Nucl. Phys. B359 (1991) 283; S. Dawson and R. Kauffman, Phys. Rev. D49 (1994) 2298; D. Graudenz, M. Spira and P. M. Zervas, Phys. Rev. Lett. 70 (1993) 1372
- [12] A. Djouadi and P. Gambino, Phys. Rev. Lett. 73 (1994) 2528
- [13] F. Hoogeveen, Nucl. Phys. B259 (1985) 19
- [14] N. G. Deshpande and E. Ma, Phys. Rev. D18 (1978) 2574; H. Georgi, Hadronic Journal 1 (1978) 155; H. E. Haber, G. L. Kane and T. Sterling, Nucl. Phys. B161 (1979) 493; J. F. Donoghue and L.-F. Li, Phys. Rev. D19 (1979) 945; L. F. Abbott, P. Sikivie and M. B. Wise, *ibid* D21 (1980) 1393; B. McWilliams and L.-F. Li, Nucl. Phys. B179 (1981) 62

Figure Captions

Fig. 1 The two-loop diagrams are obtained by attaching in all possible ways the two photon lines onto the diagram shown here. Solid and dashed lines represent fermion and scalar fields respectively.

Fig. 2 The two-loop diagrams to be computed here. Wavy lines represent photon fields.

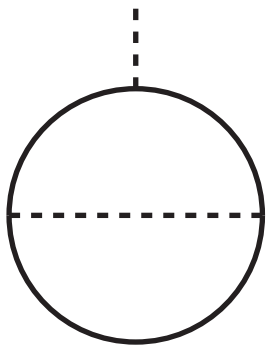


Fig. 1
Phys. Lett. B
Yi Liao

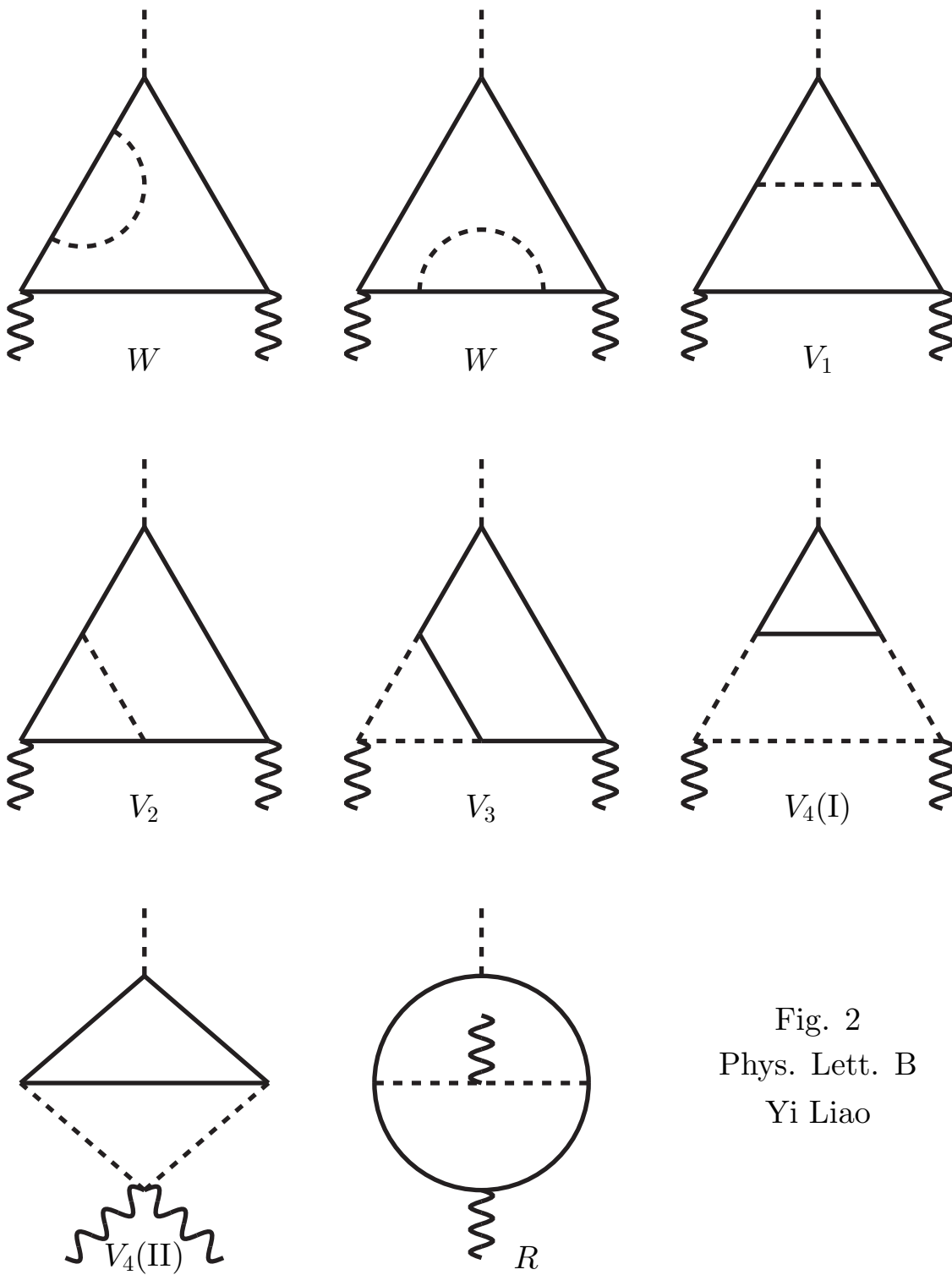


Fig. 2
Phys. Lett. B
Yi Liao